

## 5.

# Elastic-plastic stability of FML panel and columns of open and closed cross-section

### 5.1. Introduction

In the last few decades of the past century a rapid development of research on post-buckling behaviour of thin-walled structures in the elastic and elastic-plastic range until fracture took place. There are numerous publications concerning mainly singular isolated plates of different isotropic material properties. There are relatively few works dedicated to plate structures made of composite and/or laminate materials [5.2÷5.4, 5.7, 5.16]. In the last years, due to widespread of professional Finite Element Method software application, several publications appeared where full force-shortening curves of structures were determined. It concerns structures with a complex cross section made of different materials - also including orthotropic material [5.9, 5.14, 5.15].

In few works [5.6, 5.7, 5.13] the authors show the solution to the stability problem of thin-walled columns made of isotropic and orthotropic materials in elastic-plastic range. In the current study analogous issue for multi-layered materials of Fiber Metal Laminate type is considered.

Fiber Metal Laminates (FMLs) are hybrid materials, built of thin layers of metal alloy divided by layers of fiber reinforced epoxy resin. These materials are manufactured by bonding composite plies to metal ones mostly in an autoclave process. FMLs, when refers to metal layers, can be divided into FMLs based on aluminium alloys (ARALL - laminated with aramid fibers, GLARE - glass fibers, CARALL - carbon fibers) and others. Nowadays materials such as GLARE grades (glass fiber/aluminium) due to their very good fatigue and strength properties combined with the low density have been finding increasing application in an aircraft industry [5.17].

GLARE consists of alternate aluminium sheets and unidirectional high-strength glass fiber layers pre-impregnated with adhesive. Usually each glass composite layer is composed of a certain number of unidirectional (UD) plies which are stacked either unidirectionally, in a cross-ply or angle-ply arrangement. The number of layers, plies orientation and the stacking sequence of the UD plies in the entire FML panel depend on the GLARE grade. For

example, a GLARE 2 has two UD plies in a particular composite layer with the same 0-degree orientation, while a GLARE 3 has two mutually perpendicular UD plies (cross-ply arrangement). The most common type of aluminium applied in GLARE is 2024-T3 Alloy.

In current investigation it is assumed that the material of particular structure is GLARE 3 [5.10, 5.11] with an even number of glass reinforced layers, whereas the outer layers are always of aluminium. Thus the number of glass prepreg layers is always one less than the number of metallic ones. The overall laminate is symmetric with reference to the midplane. The thickness of each UD GFRP ply is 0.125 mm, so that the doubled prepreg layers of both Glare 2 and 3 grades have a total thickness of 0.25 mm.

The orthotropic glass fiber prepreg properties of a 0/90 degree (cross-ply) combination allow in the conducted here analysis to consider the composite doubled layer as one isotropic layer. Furthermore, the small anisotropy of the rolled aluminium sheet observed only for yield limits is not taken into account.

The overall dimensions of considered structures are chosen in such a way that the stability loss occurs in the elastic-plastic range for aluminium layers. Elastic-plastic moduli are used for the aluminium layers in combination with the Ramberg-Osgood (RO) curve fitting method for the stress-strain behaviour [5.7, 5.14].

When the plate structure made of GLARE is subjected to in-plane uniform compression in the elastic-plastic range of stresses, the buckling occurs in such a way that the aluminium layers become plastic but the glass fiber layers remain elastic. Therefore the behaviour of such structures differs significantly from the behaviour of pure aluminium ones.

## **5.2. Method of solution**

The problem of buckling in the elastic-plastic range of thin-walled FML columns, axially uniformly compressed, is examined using the analytical-numerical method (ANM) elaborated for the analysis of the elastic stability of multi-layered thin-walled columns [5.8]. The constitutive relationships between stress and strain for a singular elastic-plastic component layer is derived on the basis of the J2-deformation theory of plasticity (i.e. DT) or the J2-flow theory (incremental theory of plasticity i.e. IT) for Ramberg-Osgood formula.

An assumed for consideration material of FML metallic layers in the elastic range is simply defined as:

$$\sigma = E\varepsilon \quad \text{for} \quad \sigma \leq \sigma_0 \quad (5.1)$$

whereas the elastic-plastic stress-strain behaviour of FML aluminium layer is described by a Ramberg-Osgood representation of the following type:

$$\sigma = \frac{(E - E_y)\varepsilon}{\left[1 + \left(\frac{(E - E_y)\varepsilon}{\sigma_y}\right)^N\right]^{\frac{1}{N}}} + E_y\varepsilon \quad \text{for } \sigma \geq \sigma_0 \quad (5.2)$$

where:  $\sigma$  - stress,  $\varepsilon$  - strain,  $E$  - Young's modulus,  $\sigma_0$  - proportional limit,  $\sigma_y$  - conventional yield limit,  $E_y$  - tangent modulus corresponding to the yield limit  $\sigma_y$ ,  $N$  - exponent in the Ramberg-Osgood formula. The orthotropic composite layers are assumed to have elastic properties due to linear stress-strain characteristic up to fracture.

For any orthotropic plate the constitutive relationships for the elastic range and the elastic-plastic range have very similar or even identical form (Eq. 5.3):

<b>Elastic range</b>	<b>Inelastic range</b>	
$\sigma_x = K_{11}\varepsilon_x + K_{12}\varepsilon_y$	$\sigma_x = A_{11}\varepsilon_x + A_{12}\varepsilon_y$	
$\sigma_y = K_{12}\varepsilon_x + K_{22}\varepsilon_y$	$\sigma_y = A_{12}\varepsilon_x + A_{22}\varepsilon_y$	(5.3)
$\tau_{xy} = K_{33}\gamma_{xy}$	$\tau_{xy} = A_{33}\gamma_{xy}$	

Comparing the appropriate coefficients in both relations the instantaneous conventional parameters of 'elastic composite' for particular layers of entire FML structure can be found out. Thus the problem of inelastic stability of FML structures can be investigated in the analogous way as the problem of elastic composite structures. The coefficients  $A_{11} - A_{33}$  (Eq. 5.3) determined on the basis of the  $J_2$ - deformation or  $J_2$ - flow theory of plasticity depend on the appropriate Young's modulus, secant and tangent moduli for the considered material layer characteristics in the inelastic range.

The analysed problem is solved in a numerical way. The elastic problem is solved by the asymptotic Koiter's theory [5.5], formulated by Byskov and Hutchinson [5.1]. The solution of the first order approximation enables one to determine the values of buckling global and local loads and the corresponding buckling modes. This analytical-numerical method [5.7, 5.8, 5.12] created to solve the elastic problem is applied here to calculate critical load values and buckling modes for inelastic thin-walled FML columns and panels. For a given geometrical parameters, material data constants of particular FML layer and for the assumed number of buckling half-waves, the elastic buckling stress for the

considered composite structure is calculated. The most important advantage of this method is that it enables one to describe a complete range of a buckling behaviour of thin-walled structures from a global (i.e. flexural, flexural-torsional, lateral, distortional buckling and their combinations) to a local stability, including a mixed buckling modes [5.7, 5.8, 5.12].

Furthermore, a zero value of the function  $f = f(\sigma - \sigma_e)$  is searched to apply the method of secants, where  $\sigma_e$  is the value of the critical stress of the “elastic orthotropic” structure. During the computations it is assumed that  $\sigma \approx \sigma_e$ , when  $(\sigma - \sigma_e) \cdot 100\% / \sigma \leq 0.01\%$ .

The proposed method allows to consider the transition of buckling mode together with the increase of loading as distinct from the usual assumption that the elastic-plastic buckling mode is analogical to the elastic one.

For a given geometrical parameters, material constants of each FML layer and for the assumed number of buckling half-waves the elastic buckling stress for the considered composite structure is then calculated.

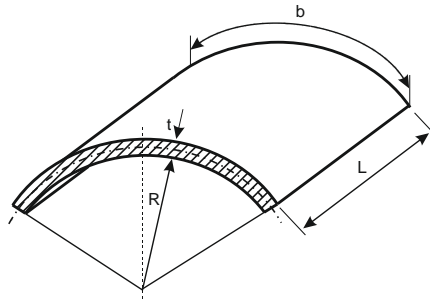


Fig. 5.1. Cylindrical shallow panel geometry

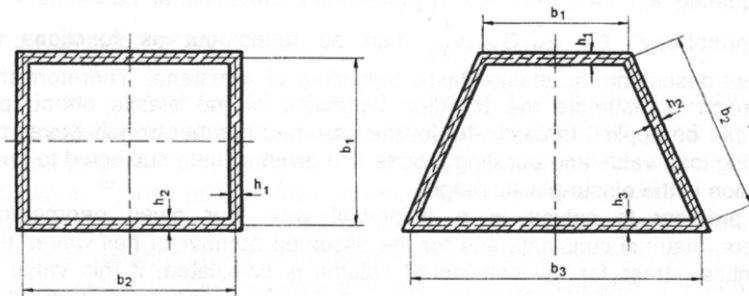


Fig. 5.2. Closed cross-sections analysed columns

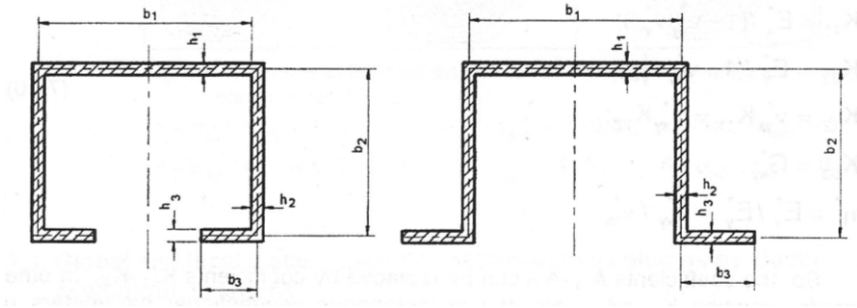


Fig. 5.3. Open cross-sections analysed columns

### 5.3. Some results of calculations

As some examples of proposed method of solution to the elastic-plastic problem of thin-walled FML hybrid composite structure a shallow cylindrical panel and a complex plate structure has been considered (Fig. 5.1÷5.3). It was assumed that the loaded edges of considered structure are simply supported at both ends. In order to account for all modes of global, local and coupled buckling, a plate model of thin-walled structure has been employed. As it was mentioned previously the overall dimensions of selected structures are chosen in such a way that the stability loss occurs in the elastic-plastic range for aluminium layers.

In presented work the detailed analysis was performed for the four chosen FML members which overall and cross-section parameters were as follows:

- a cylindrical panel simply supported along all edges subjected to axial compression (Fig. 5.1):  $R = 430$  mm,  $L = 860$  mm,  $b = 430$  mm,
- a beam/column profile with a square cross-section (Fig. 5.2a) and  $L = 1300$  mm,  $b = 130$  mm,
- a beam/column profile with a trapezoidal cross-section (Fig. 5.2b) and  $L = 1300$  mm,  $b_1 = 100$  mm,  $b_2 = 140$  mm,  $b_3 = 140$  mm,
- a beam/column profile with a top-hat (Fig. 5.3a) and a lip channel cross section (Fig. 5.3b);  $L = 1300$  mm,  $b_1 = 130$  mm,  $b_2 = 65$  mm,  $b_3 = 15$  mm.

In all cases  $L$  indicates the column length. Constructions under investigation are built of alternate aluminium sheets and unidirectional high strength glass fiber layers so this stacking corresponds to GLARE 3 grade with 2024-T3 sheets [5.11, 5.18]. The total number of layers in considered material equals 13 what leads to the total wall thickness of column/panel wall equal to  $t = 4.3$  mm where

the thickness of singular aluminium sheets equals 0.4 mm and particular doubled fiber layer 0.25 mm. Mechanical properties of both isotropic layers are presented below in Table 5.1 [5.10, 5.18].

Table 5.1. Material data of GLARE 3-7/6-0.4 (13 layers) [5.18]

Material data of GLARE 3-7/6-0.4	Elastic properties			Plastic properties		
	Young's modulus	Poisson's ratio	Proportional limit	Yield limit	Tangent modulus	Exponent in Eq. (3)
	$E$	$\nu$	$\sigma_0$	$\sigma_Y$	$E_Y$	$N$
	[GPa]	[-]	[MPa]	[MPa]	[MPa]	[-]
Al 2024-T3	700	0.3	170	290	12.1	1.8
Prepreg	30.75	0.144	-	-	-	-

Obtained results of the critical stress  $\sigma_{cr}$  calculations for the considered thin-walled FML structures (Figs. 5.1÷5.3) are shown in Figs. 5.4,5.7,5.10,5.13,5.17, respectively. Applied into the analysis three plasticity theories are distinguished in these figures as: elastic theory EL, J2-deformation theory DT and J2-incremental theory IT. For considered FML's cross-sections a stability loss can occur under symmetry (S) and anti-symmetry (A) conditions along symmetry axis of the cross-section. In the plots determined critical stress values are presented as a function of the number of half-waves  $m$  formed in the longitudinal direction. The lowest values of  $\sigma_{cr}$  are summarized in Tables 5.2÷5.6. The buckling modes of analysed FML structures are also presented in Figs. 5.5,5.6,5.8,5.9,5.11,5.12,5.14÷5.16,5.18÷5.20.

### 5.3.1. Cylindrical panel

In Figs. 5.4÷5.6 and Table 5.2 computation results for the cylindrical shallow panel are presented. According to defined above geometrical data analysed panels were of a short type because  $L/R=2$  and  $R/b=1$ , respectively.

The lowest values of critical stresses  $\sigma_{cr}$  were obtained for  $m=1$  in the case when the symmetry conditions at symmetry axis (i.e. S) were assumed, while for the assumption of asymmetry conditions (A) the number of half-waves was  $m=2$ . Determined values of critical stresses  $\sigma_{cr}$  for elastic-plastic range are lower than for elastic material behaviour. For deformation theory (DT) lower values of critical stresses were obtained in comparison to incremental theory (IT). This is a general, well-known from the literature relationship of results for both theories of elastic-plastic formulation.

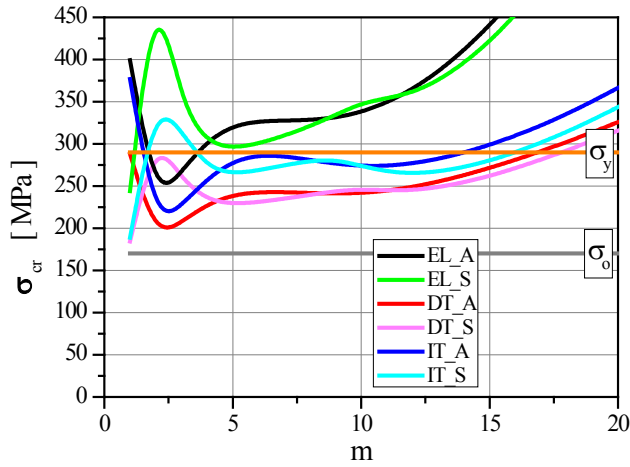


Fig. 5.4. Buckling stress  $\sigma_{cr}$  versus number of half-waves  $m$  for symmetry and antisymmetry conditions imposed along cross-section symmetry axis for shallow panel ( $\sigma_y$  - aluminum yield limit,  $\sigma_0$  - proportional limit)

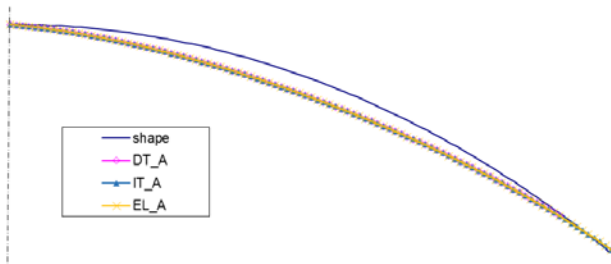


Fig. 5.5. Shapes of local antisymmetric (A) buckling modes for elastic (EL) and inelastic range (DT, IT) for panel

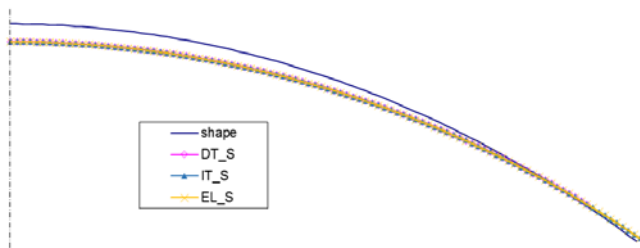


Fig. 5.6. Shapes of local symmetric (S) buckling modes for elastic (EL) and inelastic range (DT, IT) for panel

Revealed local buckling modes (Figs. 5.5, 5.6) of all three considered plasticity theories are very similar for each other for both assumed symmetry conditions at symmetry axis.

Table 5.2. Panel buckling stress and modes

Elastic range EL		Elastic-plastic range				Conditions along symmetry axis of cross-section
		DT		IT		
$\sigma_{cr}$ [MPa]	$m$	$\sigma_{cr}$ [MPa]	$m$	$\sigma_{cr}$ [MPa]	$m$	
244	1	184	1	188	1	S
233	2	190	2	205	2	A

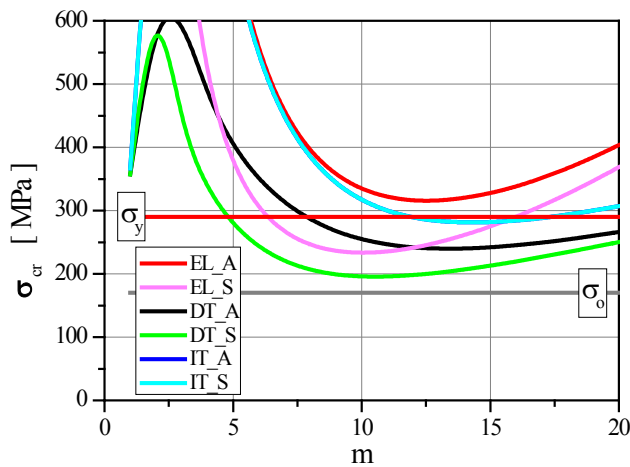


Fig. 5.7. Plots of buckling stress  $\sigma_{cr}$  versus number of half-waves  $m$  for a column of square cross-section

### 5.3.2. Closed cross-sections

In the following analysis the length of considered columns was assumed as  $L = 1300$  mm. Thus for these overall dimensions (Fig. 5.2) only local buckling modes should be considered due to significantly higher values of global buckling critical stresses in comparison to the yield limit  $\sigma_y$  (see Table 5.1).

#### *Square cross-section*

The plots in Fig. 5.7 present critical stress values  $\sigma_{cr}$  for the square cross-section from Fig. 5.2a. Particular curve corresponds to particular plasticity theory

and gives the  $\sigma_{cr}$  value as a function of half-waves number in longitudinal direction of the compressed column. In Table 5.3 the lowest values of critical stresses for considered symmetry conditions on symmetry axis are shown for comparison. Critical stress values  $\sigma_{cr}$  for symmetry conditions (S) are lower than for anti-symmetry conditions, as it was expected. The lowest value of critical stress  $\sigma_{cr}$  was obtained with deformation theory (DT) application. From Table 5.3 it is clearly visible that the number of half-waves corresponding to the lowest value of  $\sigma_{cr}$  is different for elastic theory (i.e.  $m=14$ ) from those of deformation theory (i.e.  $m=13$ ). Both local buckling modes determined for considered theories are very similar for assumed boundary conditions (Figs. 5.8, 5.9).

Table 5.3. Square cross-section

Elastic range EL		Elastic-plastic range				Conditions along symmetry axis of cross-section
		DT		IT		
$\sigma_{cr}$ [MPa]	$m$	$\sigma_{cr}$ [MPa]	$m$	$\sigma_{cr}$ [MPa]	$m$	
232	10	195	10	219	11	S
315	13	239	13	280	14	A

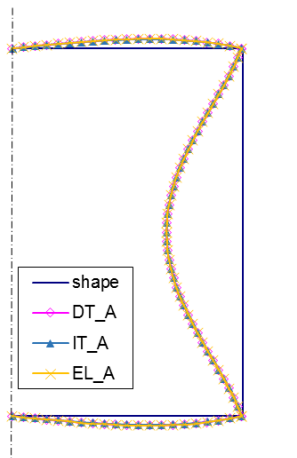


Fig. 5.8. Shapes of local antisymmetric (A) buckling modes for elastic (EL) and inelastic range (DT, IT) for square cross-section

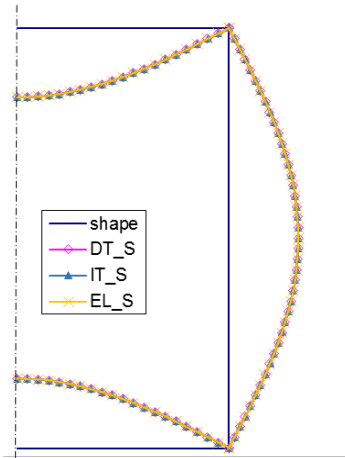


Fig. 5.9. Shapes of local symmetric (S) buckling modes for elastic (EL) and inelastic range (DT, IT) for square cross-section

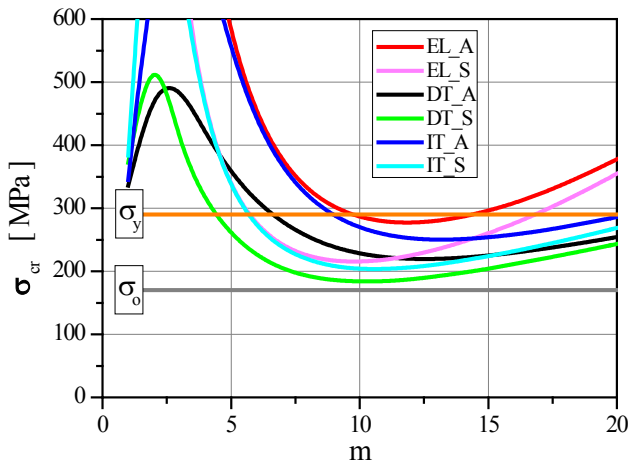


Fig. 5.10. Buckling stresses  $\sigma_{cr}$  versus number of axial half-waves  $m$  for trapezoidal cross-section

### ***Trapezoidal cross-section***

For the trapezoidal cross-section from Fig. 5.2b, there are critical stress values  $\sigma_{cr}$  as a function of half-waves number in longitudinal direction presented in Fig. 5.10 for all considered plasticity theories. Further, in Table 5.4 the lowest values of critical stresses for considered boundary conditions on symmetry axis are given. The local buckling modes for assumed boundary conditions are shown

in Fig. 5.11 and 5.12. The conclusions from the elastic-plastic analysis of FML columns of the trapezoidal cross-section are very similar to the previous comments formulated for the square cross-section FML column. When the final results of square and trapezoidal cross-section columns are compared one can observe that the critical stress values are lower for a trapezoidal-cross section column.

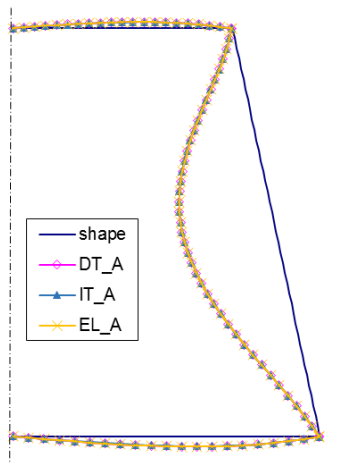


Fig. 5.11. Shapes of local antisymmetric (A) buckling modes for elastic and inelastic range for trapezoidal cross-section

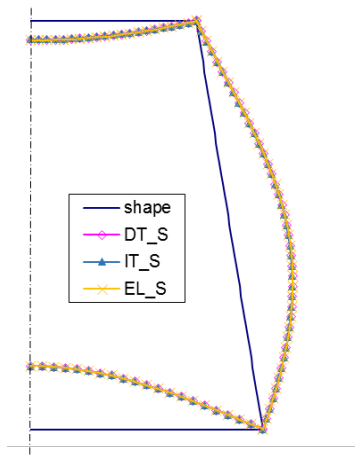


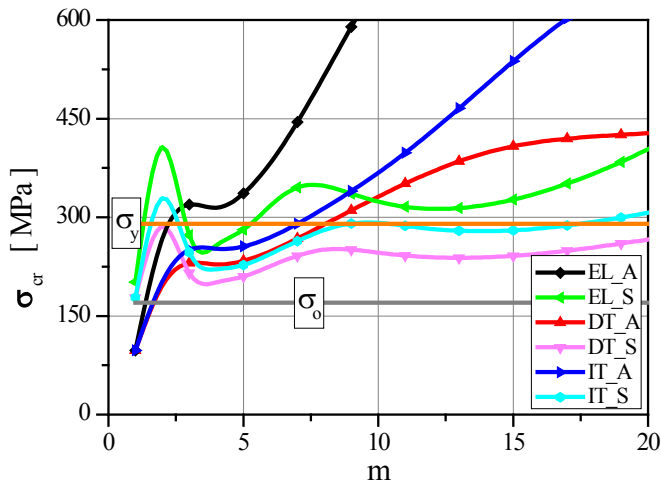
Fig. 5.12. Shapes of local symmetric (S) buckling modes for elastic and inelastic range for trapezoidal cross-section

Table 5.4. Trapezoidal cross-section results

Elastic range EL		Elastic-plastic range				Conditions along symmetry axis of cross-section
		DT		IT		
$\sigma_{cr}$ [MPa]	$m$	$\sigma_{cr}$ [MPa]	$m$	$\sigma_{cr}$ [MPa]	$m$	
214	10	183	10	203	11	S
276	12	219	12	249	13	A

### 5.3.3. Open cross-sections

In the case of investigated open cross-section columns/profiles (presented in Fig. 5.3) i.e. top hat and lipped channel, for assumed overall dimensions all global buckling modes should be examined during the analysis. Thus flexural mode (S), distortional-flexural mode (S), flexural-torsional mode (A), distortion-flexural-distortional mode (A)) and local buckling mode including distortional-local modes, should be taken into account. Therefore additional indication is introduced for open cross-section profiles - global buckling mode (i. e.  $m=1$ ) is denoted by G and local buckling mode (i.e.  $m \geq 1$ ) by L.

Fig. 5.13. Buckling stresses  $\sigma_{cr}$  versus number of axial half-waves  $m$  for top hat

#### *Top hat*

For the top hat cross-section columns/profiles (Fig. 5.3a) results of critical stresses as a function of half-waves number  $m$  are presented in Fig. 5.13. The lowest values of global and local critical stresses  $\sigma_{cr}$  are shown also in Table 5.5.

As it can be seen in this case a flexural-torsional global buckling mode (i.e.  $m = 1, A$ ) took place in the elastic range because the following relationship is fulfilled  $\sigma_{cr} = 97MPa < \sigma_0 = 170MPa$ . While a flexural buckling is observed in the elastic-plastic range (i.e.  $m = 1, S$ ). Following this observation the flexural global buckling modes could be named as "pure bending" (Fig. 5.14) while anti-symmetry mode for elastic range is a distortional-flexural-torsional mode because the lips are not perpendicular to the flanges (see EL\_A\_G curve in Fig. 5.14).

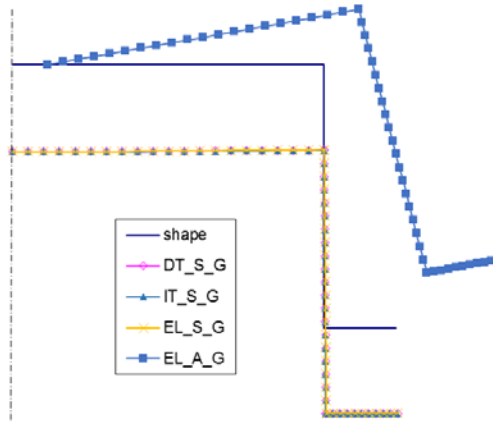


Fig. 5.14. Shapes of global buckling modes for top hat

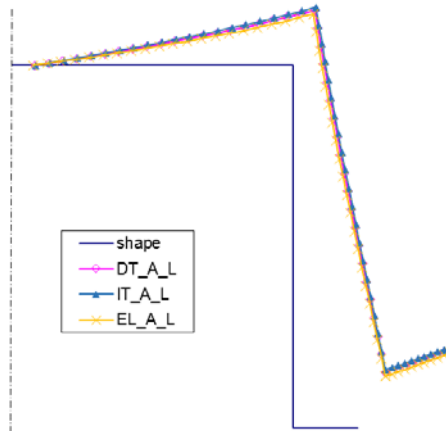


Fig. 5.15. Shapes of local anti-symmetric (A) buckling modes for a top hat profile

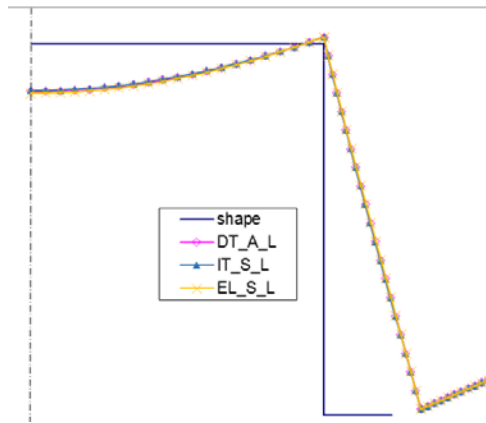


Fig. 5.16. Shapes of local symmetric (S) buckling modes for top hat profile

It can be seen in Table 5.5 that the value of the local critical stress  $\sigma_{cr}$  of symmetric mode (i.e.  $m = 4$ , S) for elastic range is lower in comparison to a local anti-symmetric mode buckling stress (i.e.  $m = 2$ , A) for elastic range. However, values of  $\sigma_{cr}$  for both elastic-plastic formulations and antisymmetrical modes are lower than the symmetric ones. For  $m \geq 1$  buckling modes are distortional-local modes for both boundary conditions (Figs. 5.15, 5.16). Buckling modes are practically the same for each of applied theories.

Table 5.5 Top hat results

Elastic range EL		Elastic-plastic range				Conditions along symmetry axis of cross-section
$\sigma_{cr}$ [MPa]	$m$	DT		IT		
		$\sigma_{cr}$ [MPa]	$m$	$\sigma_{cr}$ [MPa]	$m$	
201	1	177	1	178	1	S
257	4	201	4	220	4	S
97	1	-	-	-	-	A
267	2	196	2	202	2	A

### ***Lipped channel***

In Fig. 5.17 critical stress values  $\sigma_{cr}$  as a function of half-waves number  $m$  are presented for the FML column of lipped channel cross-section. Table 5.6 shows as well the lowest values of global and local  $\sigma_{cr}$  for both considered boundary conditions while corresponding to them buckling modes are given in Figs. 5.18÷5.20.

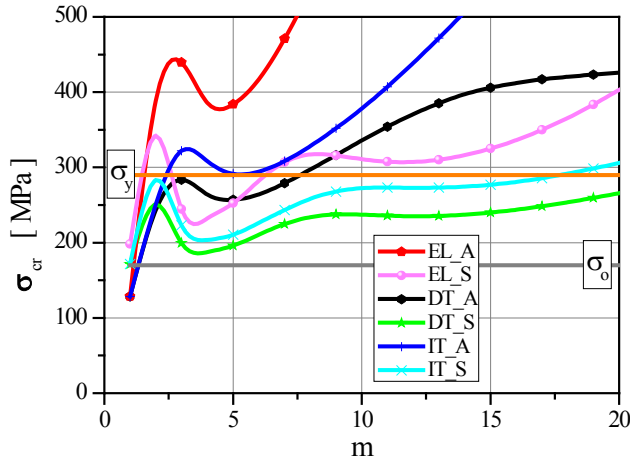


Fig. 5.17. Buckling stresses  $\sigma_{cr}$  versus number of axial half-waves  $m$  for lip channel column

The lowest value of critical stresses  $\sigma_{cr} = 128$  MPa corresponds to a global flexural-torsional mode (i.e.  $m=1$ , A) in elastic range (see EL\_A\_G line in Fig. 5.18). The global buckling stress value  $\sigma_{cr} = 198$  MPa ( $m=1$ , S) corresponds to a distortional-flexural buckling mode for elastic range (Fig. 5.18). Symmetric global buckling modes are similar for considered constitutive theories. Local buckling stress values are lower for symmetric modes in comparison to anti-symmetry ones.

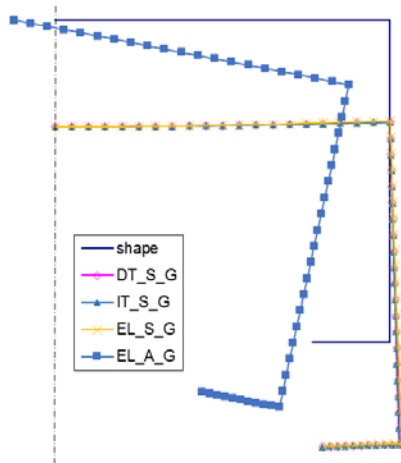


Fig. 5.18. Shapes of global buckling modes for lip channel

Presented in Figs. 5.19 and 5.20 buckling modes are of distortional-local symmetric and anti-symmetric type. It should be emphasized that local symmetric buckling modes (Fig. 5.20) differ slightly between themselves at the junction of flanges with the lips. In works [5.6, 5.11] for one-layered isotropic and orthotropic structures there was a lot of variety local and global buckling modes obtained which differed significantly between themselves for elastic and elastic-plastic range.

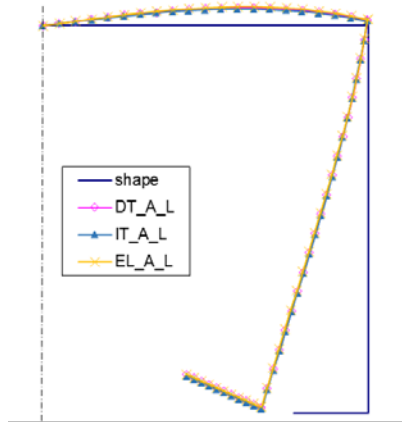


Fig. 5.19. Shapes of local anti-symmetric (A) buckling modes for lip channel

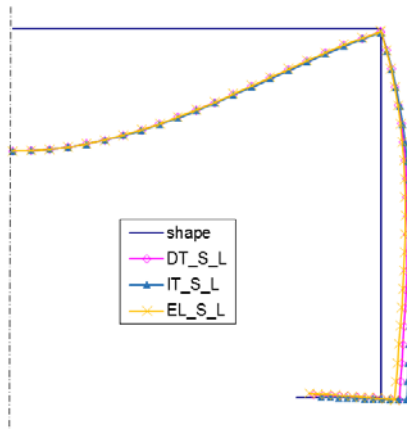


Fig. 5.20. Shapes of local symmetric (S) buckling modes for lip channel

As it can be seen from presented in current work buckling modes for FML multi-layered structures determined buckling modes differ at least slightly between themselves because particular elastic glass fibre layers work within elastic range. Thus mechanical properties of glass fibre layer remain unchanged

in elastic-plastic range of entire FML wall, when aluminium layer changes own properties from isotropic to orthotropic. It makes that multi-layered structures are not as sensitive to changes of buckling modes as one-layered structures. The latter change their mechanical properties across whole thickness in the elastic-plastic range [5.6, 5.13].

Table 5.6. Lipped channel results

Elastic range EL		Elastic-plastic range				Conditions along symmetry axis of cross-section
		DT		IT		
$\sigma_{cr}$ [MPa]	$m$	$\sigma_{cr}$ [MPa]	$m$	$\sigma_{cr}$ [MPa]	$m$	
198	1	176	1	177	1	S
232	4	187	4	203	4	S
128	1	-	-	-	-	A
383	5	256	5	291	5	A

## 5.4. Conclusions

In work the comparison of critical stresses for thin-walled FML structures in elastic and elastic-plastic range is presented. Two plasticity theories were considered i.e. J2-deformation theory and J2-incremental theory. The lowest values of critical stresses for all analysed structures were obtained in elastic-plastic range for the deformation theory. It is fully consistent with results presented in literature survey. Moreover it ought to be pointed out that:

- the solutions given here are valid in the cases of the uniform compression of the thin-walled FML structure. Other types of loadings would need further investigation,
- the usual assumption, made in many works in the field, that the buckling modes in the elastic and elastic-plastic range are identical cannot be true in some cases,
- it should be noted that the buckling modes in elastic and elastic-plastic range can be not always cover-up.

### *Acknowledgment*

This contribution is a part of the project funded by the National Science Centre Poland, allocated on the basis of the decision No. 2012/07/B/ST8/0409.

## 5.5. References

- 5.1 Byskov E., Hutchinson J.W., Mode interaction in axially stiffened cylindrical shells, *AIAA J.*, 15 (7), 1977, pp. 941-48.
- 5.2 Grądzki R., Kowal-Michalska K., Post-buckling analysis of elastic-plastic plates basing on the Tsai-Wu criterion, *JTAM*, 4, 37, 1999, pp. 893-908.
- 5.3 Grądzki R., Kowal-Michalska K., Ultimate load of laminated plates subjected to simultaneous compression and shear, *The Archives of Mechanical Engineering*, XLVIII, 3, 2001, pp. 249-264.
- 5.4 Grądzki R., Kowal-Michalska K., Stability and ultimate load of three layered plates - a parametric study, *Engineering Transactions*, 51,4, 2003.
- 5.5 Koiter W.T., General theory of mode interaction in stiffened plate and shell structures, *WTHD Report 590*, Delft 1976, 41.
- 5.6 Kołakowski Z., Kowal-Michalska K., Kędziora S., Determination of inelastic stability of thin walled isotropic columns using elastic orthotropic plate equations, *Mechanics and Mechanical Engineering*, 1997, 1 (1), pp. 79-90.
- 5.7 Kolakowski Z., Kowal-Michalska K. (Eds.), Selected problems of instabilities in composite structures, *A Series of Monographs*, Technical University of Lodz, Poland, 1999.
- 5.8 Kolakowski Z., Krolak M., Modal coupled instabilities of thin-walled composite plate and shell structures, *Composite Structures*, 2006, 76, pp. 303-313.
- 5.9 Kołakowski Z., Kowal-Michalska K. (Eds.), Statics, dynamics and stability of structures, Vol. 2, Statics, dynamics and stability of structural elements and systems, Lodz University of Technology, *A Series of Monographs*, Lodz 2012.
- 5.10 Kowal-Michalska K., Kolakowski Z., Inelastic buckling of thin-walled FML columns by elastic asymptotic solutions, *39<sup>th</sup> Solid Mechanics Conf. Zakopane*, Poland, 2014.
- 5.11 Kolakowski Z., Kowal-Michalska K., Mania R.J., Global and local elastic-plastic stability of FML columns of open and closed cross-section, *Proc. of Polish Congress of Mechanics*, 2015, pp. 907-908.
- 5.12 Kolakowski Z., Mania J.R., Semi-analytical method versus the FEM for analysis of the local post-buckling. *Composite Structures*, 97, 2013, pp. 99-106.
- 5.13 Kowal-Michalska K., Kołakowski Z., Kędziora S., Global and local inelastic buckling of thin-walled orthotropic columns by elastic asymptotic solutions, *Mechanics and Mechanical Engineering*, 1998, 2 (2) pp. 209-231.
- 5.14 Kowal-Michalska K., Stany zakrytyczne w obszarach sprężysto-plastycznych konstrukcji płytowych, Lodz University of Technology, *A Series of Monographs*, Lodz 2013 /in Polish/.
- 5.15 Kowal-Michalska K., Problem of modeling in the non-linear stability investigation of thin-walled plated structures, Part II - Elasto-plastic range, pp. 157-180, in monograph "Mathematical models in continuum mechanics" (Eds. K. Wilmański, B. Michalak, J. Jędrysiak), Lodz University of Technology, *A Series of Monographs*, 2011.

- 5.16 Mania J.R., Kolakowski Z., Bienias J., Jakubczak P., Majerski K., Comparative study of FML profiles buckling and postbuckling behaviour under axial loading, *Composite Structures*, Vol. 134, 2015, pp. 216-225.
- 5.17 Vermeeren C. (ed.), *Around GLARE, A new aircraft material in context*, Kluwer Academic Publishers. 2004.
- 5.18 Wittenberg T.C., de Jonge A. Plasticity correction factors for buckling of flat rectangular Glare plates. *DUT, Int. Council of the Aeronautical Sciences*, 2002, 482.1-482.13.